PAPER

Check for updates

Pseudo second order kinetic expression to predict the kinetics of the anomalous crystal growth of curcumin in impure solution

Mahmoud Ranjbar, [iD] †[a] Mayank Vashishtha,[a] Srinivas Gadipelli, [iD] [b] Kirankumar Ramisetty,[c] Gavin Walker,[a] Dan J. L. Brett [iD] [b] and K. Vasanth Kumar [iD] †*[ad]

Crystals growing *via* nonclassical crystallisation pathways often lose the shape factor and the mechanisms involved are often anomalous. This makes it difficult to predict the crystal growth kinetics using the conventional crystal growth kinetic models. A new pseudo second order growth kinetic expression to predict the anomalous growth behaviour of curcumin crystals is introduced. This model also allows several important parameters relevant to the kinetics of the crystal growth, such as mass crystallised with respect to time, overall crystal growth kinetic constant, the maximum number of active sites involved in the crystal growth process and the initial crystal growth rate, to be obtained. According to the pseudo second order kinetics, the activation energy for the nonclassical crystal growth of curcumin was found to be ~69 kJ mol^{-1}, which seems to agree with the activation energy for the classical crystal growth of organic compounds reported in the literature. The total number of active sites involved in the crystal growth process was found to be ~10^{22} per gram of the seeds.

1. Introduction

During crystal growth, ideally, each crystal facet grows at a different rate and thus retains the shape factor.[1,2] A major use of crystallisation is to purify the compounds and crystallisation is the most widely used unit operation to purify several active pharmaceutical ingredients.[3,4] The concept of purifying an active pharmaceutical ingredient (API) is simple. Typically, a crude product will be dissolved in a suitable solvent at elevated temperature followed by the cooling of the solution to create supersaturation. Once the solution reaches the working temperature, a certain weight percentage of seed will be added. The seed crystals will grow at the expense of supersaturation.

The crystal growth kinetics of such perfect crystal growth processes can be modelled using the classical mechanistic models like the Burton–Cabrera–Frank,[5] spiral nucleation,[6,7] surface diffusion,[5] and multiple nucleation models.[1]

Alternatively, transport kinetic models like the two-step mass transfer model can be used to predict the growth kinetics and the rate-limiting step of the classical crystal growth process.[1,7] Other kinetic models used to model the crystal growth kinetics include the surface diffusion and surface integration based models.[8] During crystal growth, in some cases, the crystals may lose their shape factor and can exhibit anomalous growth behaviour that cannot be modelled using conventional theoretical kinetic expressions, which rely on shape factors and assume that the crystal habit remains the same during the growth process. It is essential to develop new kinetic models that can explain the occasionally encountered non-classical crystal growth behaviour. In this work, it is shown that curcumin crystals exhibit anomalous growth behaviour during growth from their impure solutions. Curcumin is an industrially important active pharmaceutical ingredient with diverse pharmacological activities and used as an anticancer, anti-inflammatory, anti-malaria, anti-HIV agent, *etc.*[9,10] In our earlier work, we showed that curcumin crystallises *via* a non-classical crystallisation pathway and the morphology of the final crystals mostly deviate from the equilibrium (needle) habit of this compound.[11–13] In fact, this system is selected on purpose as the crystals grow *via* the non-classical pathway (discussed in detail in section 3) and currently there is no reliable mathematical model available to accurately capture the kinetics of such anomalous crystal growth behaviour. It is essential to develop a kinetic model

[a] *Synthesis and Solid State Pharmaceutical Centre, Department of Chemical Sciences, Bernal Research Institute, University of Limerick, V94 T9PX, Ireland*

[b] *Electrochemical Innovation Lab, Department of Chemical Engineering, University College London, London, WC1E 7JE, UK*

[c] *MSD Ballydine, Kilsheelan, Clonmel, Co Tipperary, E91 V091, Ireland*

[d] *Chemical and Process Engineering, School of Chemistry and Chemical Engineering, University of Surrey, Guildford, GU2 7XH, UK. E-mail: v.kannuchamy@surrey.ac.uk*

† Equal contribution.

that can capture the anomalous/or non-classical crystal growth behaviour and to predict the corresponding crystal growth kinetic constants and their activation energies. Such models are useful for the process design and in scale-up calculations.

This work shows that a simple second-order kinetic expression can accurately predict the kinetics of the non-classical growth of curcumin. It also shows that the second-order kinetic expression allows estimation of the kinetic constant, theoretical saturation limit, initial crystallisation rate and activated energy associated with the crystal growth process. Furthermore, to design the crystal growth experiments, it is essential to obtain information about the solubility, which is demonstrated using a process analytical technology tool (*in situ* Raman spectroscopy).

2. Theory: second order crystal growth kinetics

Crystals grow *via* the addition of adatoms or molecules onto the active sites available on the crystal surface. These sites are often called kink sites. According to the established Terrace–Step–Kink model, the adatoms can be directly adsorbed onto the kink sites followed by their integration. Alternatively, the adatoms will be adsorbed onto the ledges or onto the crystal surfaces followed by diffusion onto the kink sites. Using these theoretical facts as a basis, in this work, we propose the pseudo second order expression to model the nonclassical crystal growth kinetics of curcumin in isopropanol. The pseudo second order model is proposed based on the following theoretical assumptions:

(1) At any instant of time, there exist active sites on the crystal surface that can host the target molecule.

(2) At any instant of time, during the crystal growth process, at least two sites are involved in the crystal growth process.

(3) Two adatoms are adsorbed onto the active sites at any instant of time. We further assume that the crystallising compound is adsorbed onto these sites followed by its integration.

(4) The active sites will be available to host the target molecule provided that there is supersaturation.

(5) The crystal active sites cannot host the target molecule once the solution reached the solubility limit.

(6) Irrespective of the number of active sites available on the surface of the crystal, the active sites can host the target molecule only if the solution concentration is greater than the solubility concentration.

(7) As the entire crystallisation process is dictated by supersaturation, depending on the initial supersaturation, there exist a maximum number of active sites that dictate the kinetics of the crystallisation process.

(8) The process is limited by the surface integration process.

(9) Even if the crystal surface is enriched with sites, they will actively host the target molecule only if the solution

concentration is above the solubility limit. The crystal active sites cannot host the target molecule once the solution reached the solubility limit.

(10) Irrespective of the number of active sites available on the surface of the crystal, the site can host the target molecule only if the solution concentration is greater than the solubility concentration.

(11) As the entire crystallisation process is dictated by supersaturation, depending on the initial supersaturation, there exist a maximum number of active sites, M_m that dictate the crystallisation process. The parameter M_m corresponds to the total number of active sites involved in crystal growth during the depletion of concentration from its initial concentration, c_o (g L^{-1}), to solubility concentration, c^* (g L^{-1}). In other words, once all M_m (g of curcumin per g of seeds) sites are involved in the crystal growth process, then the solution concentration is assumed to reach the solubility concentration.

The crystal growth process can be expressed by the following mechanism.

$$T + AS \rightarrow T{\cdot}AS$$

where T is the target molecule that will crystallise at the expense of supersaturation and 'AS' is the active site for the target molecule.

If we assume that T_m is the total number of active sites involved during the consumption of the entire supersaturation, $\Delta C = c_o - c^*$, and the crystallisation kinetics is of second order, the rate of crystallisation can be defined as

$$dT/dt = k_v(T_m - T_t)^2$$

where Δc is the supersaturation (g L^{-1}), S is the supersaturation ratio, k_v is the crystallisation kinetic constant, T_m is the total number of sites involved in the crystallisation process, and T_t is the number of active sites involved in the crystal growth process at any time, t. The concept of crystallisation according to the assumptions made is represented using a model schematic shown in Fig. 1.

Based on the above assumptions, the crystallisation kinetics can be written as

$$dM_t/dt = k_v(M_m - M_t)^2$$

where M_t is the mass of target molecule deposited onto the active sites of the seed crystals.

The crystallisation kinetic rate expression can be written as

$$\frac{dM_t}{dt} = k_v(M^* - M_t)^2 \tag{1}$$

where k_v is the crystallisation kinetic constant, M_t is the mass crystallised onto a unit mass of seed crystals, M^* is the mass
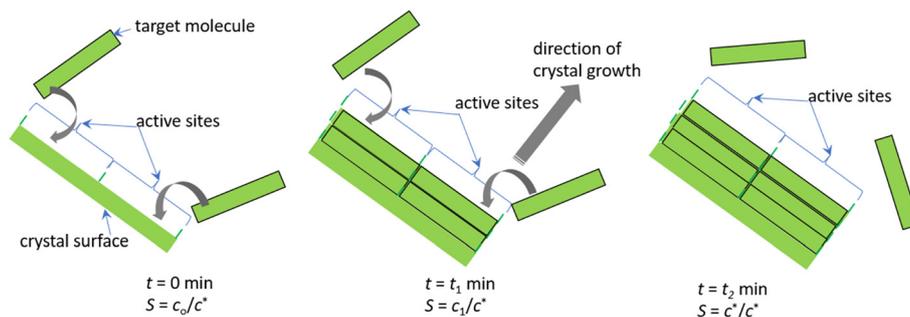
Fig. 1 A concept of the growth of a crystal facet according to the proposed kinetic model. When $t = 0$, the crystal facet is assumed to contain two active sites. Each active site will be occupied by the target molecule. After the target molecule binds to the active sites on the crystal surface and undergoes surface integration, the emerging crystal surface develops fresh active sites. These sites are capable of accommodating new target molecules, thereby promoting the expansion of the crystal facet. This process continues until the solution concentration reaches the solubility concentration. Note: $c_o > c_1 > c^*$. According to the concept diagram shown in this figure, when $t = t_1$, four sites are occupied by the target molecule leading to the growth of the crystal facet. When $t = t_2$, six sites are involved in the crystal growth process leading to the further growth of the crystal. When $t = t_2$, all the supersaturation is consumed and thus even if the crystal surface contains sites that can accommodate the target molecule, it cannot host new target molecules as the crystal surface is said to be in equilibrium with the saturated solution.

crystallised onto a unit mass of seed crystals at equilibrium (*i.e.*, once the solution reached the equilibrium).

M and M^* can be obtained from a simple mass balance given by

$$M_t = (c_o - c_t) \frac{V}{M_{seed}} \quad (2)$$

$$M^* = (c_o - c^*) \frac{V}{M_{seed}} \quad (3)$$

where V is the volume of the solvent (L) and M_{seed} is the mass of the seeds (g).

Eqn (1) can be rearranged as follows:

$$\frac{dM_t}{(M^* - M_t)^2} = k_v dt \quad (4)$$

Eqn (4) can integrated with respect to the boundary conditions, $M_t = 0$ when $t = 0$ and $M_t = M_t$ when $t = t$.

$$\frac{1}{M^* - M_t} = \frac{1}{M^*} + k_v t \quad (5)$$

Eqn (5) can be rearranged in to:

$$\frac{t}{M_t} = \frac{1}{k_v M^{*2}} + \frac{t}{M^*} \quad (6)$$

According to the linear expression shown in eqn (6), if the crystallisation kinetics follows the second order kinetics, then a plot of t/M_t *versus* t should be linear and allows prediction of the kinetic constant and the total number of sites involved in the crystallisation.

The kinetics constant k_v and M^* can be theoretically obtained using a nonlinear regression analysis by fitting the experimental crystallisation kinetics, eqn (7)

$$M_t = \frac{k_v M^{*2} t}{1 + k_v M^* t} \quad (7)$$

It can be realised from eqn (7) that the crystallisation kinetics can be captured without obtaining any information about the

shape factors of the crystals. It can predict the increase in solid concentration as a function of time, if the kinetic constant and the total number of sites involved in the crystal growth are known.

According to eqn (7), when t approaches zero, the value of M_t/t approaches the value that will be equal to the initial crystallisation rate, $v_k = k_v M^{*2}$. Thus, from the estimated k_v and M^*, it is possible to calculate the initial crystallisation rate. While the availability of active sites on the crystal surface and concentration are factors influencing crystal growth, the growth process is fundamentally governed by concentration alone. Crystals only grow when the $c > c^*$ regardless of the number of active sites, the quantity of crystals, or the surface area within the crystallizer. Thus, the proposed second-order kinetic expression has pseudo-second-order crystal growth kinetics. Earlier, a similar expression to model the growth kinetics of sucrose crystals in their supersaturated solutions was proposed by the authors.[14] It should be mentioned here that sucrose crystals grow *via* the classical crystal growth process, whereas curcumin crystals clearly tend to deviate from the classical crystal growth process. Therefore, in this study, we need to introduce additional assumptions and make certain modifications to formulate an expression that captures the nonclassical crystal growth kinetics of curcumin. Additionally, in this work, a theoretical justification for the proposed model and thus the kinetic parameters involved in the proposed expression has been included to provide more physical meaning and introduce important parameters like the initial crystallisation rate and the number of active sites involved in the crystal growth process.

3. Results and discussion

3.1. Solubility of crude curcumin

Fig. 2a shows a plot of intensity (peak height was normalised so that its values will fall within the range 0 to 1) of Raman spectral modes observed at 1251 cm^{-1}, 1431 cm^{-1} and 1601
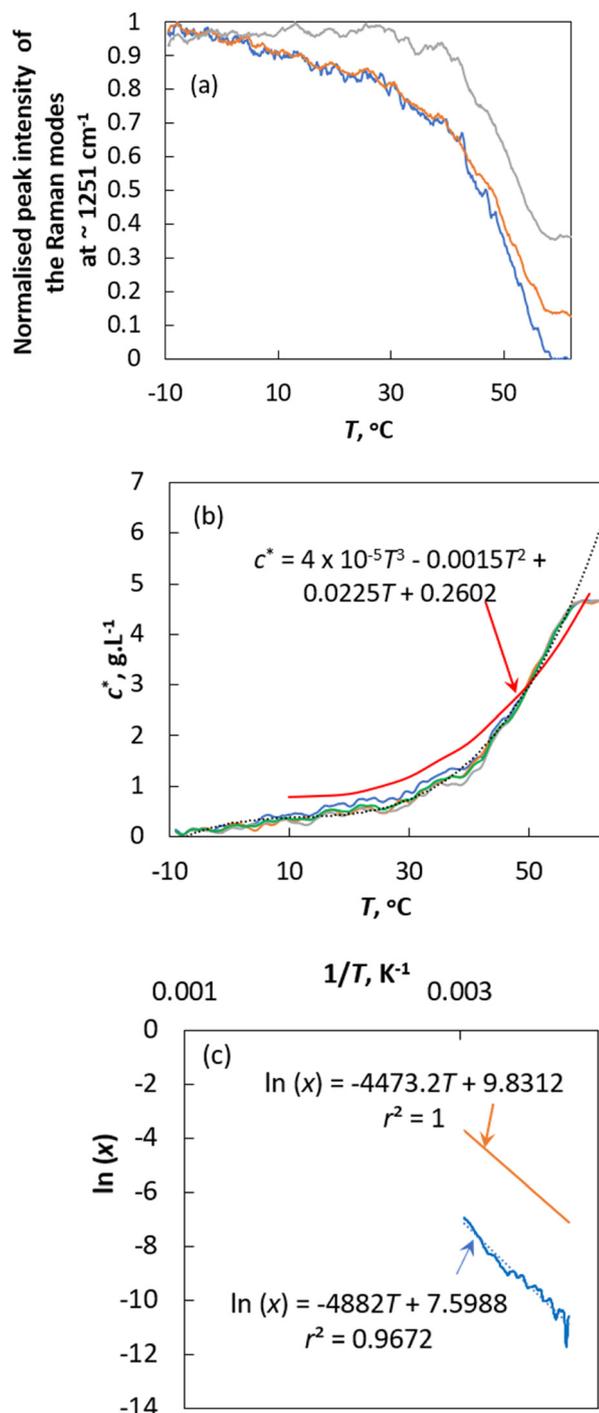
Fig. 2 (a) Normalised peak intensity of the Raman modes at ~1251 cm⁻¹ (blue line), ~1431 cm⁻¹ (orange line) and ~1601 cm⁻¹ (grey line). (b) Solubility of crude curcumin obtained from the intensity of Raman peaks (blue line: ~1251 cm⁻¹, orange line: ~1431 cm⁻¹, grey line: ~1601 cm⁻¹ and green line: average of c^* obtained based on the intensity of the peaks using eqn (8). Solubility of pure curcumin is shown by the red line. The trend line (grey dotted line) and the corresponding best-fit empirical expression is also shown in the figure. (c) Plot of ln(x) *versus* 1/T. Orange line: ideal solubility line (with corresponding expression) for crude curcumin, blue line: solubility obtained experimentally using *in situ* Raman data, and blue dotted line: trend line that best fits the experimental data. Solubility of crude curcumin as a function of temperature is deduced according to ideal solubility expression.

cm⁻¹ (refer to the Experimental section for details) as a function of solution temperature. From Fig. 2a, it can be observed that the intensity of the observed Raman modes decreases exponentially with solubility temperature, from −8.4 °C to 57.5 °C. The exponentially decreasing Raman intensity indicates that the solid concentration in the reactor decreases with increasing temperature. For temperature $T >$ 57.5 °C, there is no change in the Raman mode intensity. This essentially indicates that at 57.5 °C all the solids in the reactor are completely dissolved, and after this point, the observed Raman intensity corresponds only to the concentration of curcumin in the liquid phase. Thus, the intensity of the observed peaks for the $T \geq$ 57.5 °C region can be called as the final intensity that corresponds to the concentration of curcumin in the solvent in the fully dissolved state, I_{liquid}. Then the solubility concentration of crude curcumin can be calculated using the expression given by

$$c^* = \frac{I_{\text{o}} - I_{\text{T}}}{I_{\text{o}} - I_{\text{liquid}}} \times M_{\text{cur}} \tag{8}$$

where c^* is the solubility concentration of curcumin, I_{o} is the intensity of the Raman peak observed at −8.4 °C, I_{T} is the intensity of the Raman peak observed at any temperature, T and I_{liquid} is the intensity of the Raman peak when all the solids are dissolved. It should be mentioned that eqn (8) is valid only when the Raman intensity increases linearly with the solid concentration and the intensity of Raman does not show a significant increase as a function of concentration. Several trial experiments have been performed (the results are not shown here) and confirmed that, for the case of curcumin, the intensity of the three Raman peaks considered in this work increases linearly with solid concentration and the intensity is not influenced by the liquid concentration. Fig. 2b shows the solubility concentration obtained using eqn (8) as a function of temperature. The solubility values derived from all three Raman peaks indicated the same solubility values. Fig. 2b shows the average of the solubility obtained from the intensity of three Raman peaks as a function of temperature. This indicates that solubility values increase exponentially with temperature. The variation in the solubility as a function of temperature can follow the polynomial expression shown in Fig. 2b. Additionally, the solubility of curcumin in isopropanol was found to vary with temperature according to the expression for ideal solubility:

$$\ln(x) = \frac{\Delta H}{R}\frac{1}{T_{\text{m}}} - \frac{\Delta H}{R}\frac{1}{T} \tag{9}$$

where x is the molar fraction of CUR, ΔH is the enthalpy of fusion (J mol⁻¹), T is the solubility temperature (K), T_{m} is the melting point of CUR (K), and R is the gas constant (J mol⁻¹ K⁻¹).

According to eqn (9), a plot of ln(x) *versus* 1/T should be linear (as shown in Fig. 2c) and the enthalpy of fusion and the melting point are obtained from the slope and intercept of the linear plot. The calculated ΔH and T_{m} were about

40.58 kJ mol^{-1} and 369.46 °C. These values seem to deviate from the experimentally obtained (for crude curcumin) values of ΔH = ~38.67 kJ mol^{-1} and T_m = ~169.74 °C. For comparison purposes, the ideal solubility behaviour of curcumin is shown in Fig. 2c. The ideal solubility data was obtained using the experimentally deduced ΔH (37.19 kJ mol^{-1}) value. The experimentally obtained solubility deviates from the theoretical solubility, which can be expected as the latter one ignores the solute–solvent interactions, and it solely depends on the lattice energy of the crystal. Additionally, the ideal solubility was obtained based on the melting point of pure curcumin, whereas the experimental solubility was obtained with crude curcumin that contains >20 wt% of structurally similar impurities.

3.2. Crystal growth of crude curcumin in isopropanol

Fig. 3 shows the plot of mass of curcumin crystallised onto a unit mass of seed crystals, M_t *versus* time at three different temperatures. The morphology from scanning electron microscopy (SEM) images of the final crystals collected at the end of each crystal growth experiment is shown in Fig. 4. For comparison purposes, the morphology of the seed crystals is also shown in Fig. 4. The SEM images of seed crystals show that they are needle shaped, which is the expected crystal habit of the form I (FI) curcumin crystals.[11] Crystals obtained from the crystal growth experiments seem to retain the needle shaped habit of FI curcumin. If crystals grow following the rules of classical crystal growth, then each crystal facet should grow at a specific speed and thus theoretically the seed crystals should retain the needle habit of FI curcumin. The SEM images show the existence of

Fig. 3 Plot of mass of curcumin crystallised onto a unit mass of seed crystals *versus* time. Black lines: Kinetics predicted by the pseudo second order expression.

multiple needle shaped structures evolved from the parent seed crystals. The morphology points to the fact that the seed crystals should have grown *via* the nonclassical crystallisation pathway. The crystals collected from the crystal growth experiment performed at 15 °C show multiple filamentous structures emerging from the needle shaped seed crystals. These filamentous structures altogether look like spherulites which clearly does not resemble the needle habit of the seed crystals. Earlier, it was shown that such spherulite structures should have formed *via* growth front nucleation and low angle branching from a common point.[11] In the crystals obtained at slightly higher temperatures, 20 and 38 °C, several new structures emerged out of the parent seed crystals. However, in the experiments performed at 20 and 38 °C, the concentration of the newly evolved structures looks less dense when compared to the ones observed in the crystals obtained at 15 °C. Clearly, the temperature has a crucial role in the crystal morphology. Based on the SEM results, it is believed that lower temperature favours the growth front nucleation on the crystal surface which leads to formation of spherulites on the seed crystals that are denser when compared to the ones obtained at higher temperature. In our recent work, it was shown that curcumin crystals tend to grow *via* the formation of a few hundred thick crystal habit during the crystal growth process which acts like the growth front where new surface units evolve into filament like structures (as observed in the SEM images of crystals obtained at 15 °C – see Fig. 4a) or as needles (as observed in the SEM images obtained at 25 and 38 °C) – see Fig. 4b and c. We explained the growth process in the light of the so called repeated two-dimensional (2D) nucleation and sympathetic nucleation. The term repeated 2D nucleation refers to the growth of surface units on the parent seed crystals *via* 2D nucleation that occurs repeatedly on the crystalline surface, which usually evolves into needle shaped or filament-like structures (shown in Fig. 4a–d).

To gain further insight into the crystal growth process, the crystal population was monitored during the growth process at 15 °C using FBRM and the results are shown in Fig. 5. FBRM counts were predicted for this experiment as the SEM results show the outgrowth of more new crystalline units on the surface of the parent crystals *via* the above mentioned nonclassical crystallisation process when compared to that of the crystals obtained at other studied temperatures. Thus, it may be more likely to expect secondary nucleation (*i.e.*, birth of new crystals after the addition of seeds) at this temperature. Fig. 5 shows the plot of percentage of the crystals of different size fractions as a function of time. Fig. 5 also plots the total FBRM counts as a function of time. It is clear from Fig. 5 that the overall count of the particles obtained from FBRM remains constant. This points to the experimental fact that the crystal population remains constant and thus there is no secondary nucleation during the growth process. Another noteworthy observation is that the population of the crystals in the size fraction ranging from 100–150 mm and 150–200 mm increases with time,
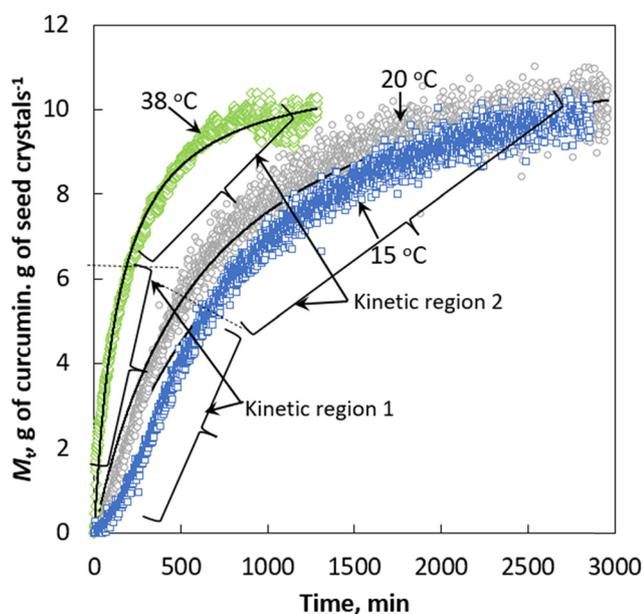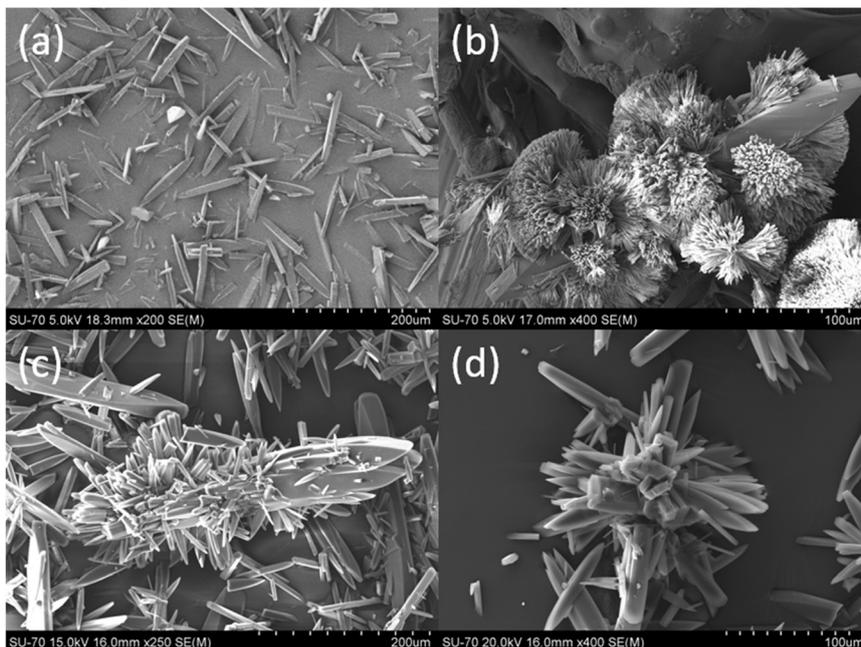
Fig. 4 SEM images of the (a) seed crystals and the final crystals obtained from the isothermal desupersaturation crystal growth experiment performed at (b) 15 °C, (c) 20 °C and (d) 38 °C. Note: The method to obtain the seed crystals can be found elsewhere.[11]

whereas the crystals in the size fraction ranging from 10–50 mm and <10 mm decreases with respect to time during the crystal growth process. This shows that the smaller crystals grow at the expense of larger crystals, which seems to be unique, unconventional and the first time it has been observed during the growth of curcumin crystals. This type of growth behaviour means that the larger crystals are ripening to promote the growth of smaller crystals, which can be termed as growth *via* sympathetic ripening, where larger crystals are dissolved to promote the growth of finer particles. Another noteworthy observation is that the total counts decrease slightly with time, and this can be attributed

to crystal agglomeration during the growth process. To summarise, the crystal growth of curcumin followed a nonclassical crystallisation pathway that leads to crystalline products with a crystal habit that is indifferent to that of the parent seed crystals. More importantly, there is no secondary nucleation, but the parent seed crystals lose the shape factor of the needle shaped crystals during the growth process. This makes it theoretically impossible to implement conventional theoretical crystal growth models that usually rely on shape factors to convert the supersaturation consumed during crystal growth. Thus, it is essential to rely on an alternate theoretical model such as the pseudo second order kinetics proposed in this work to model the crystals growing *via* the nonclassical crystal growth pathways.

In terms of the crystallisation rate, the results shown in Fig. 3 confirm that temperature plays a crucial role in the crystal growth kinetics. The higher the temperature, the faster the crystal growth rate. In terms of crystallisation kinetics, the results clearly indicate that there exist two regions in the plot of M_c versus t. Regardless of the temperature, the amount of mass deposited onto a unit mass of seed crystals was substantial during the early (first) stage of the crystal growth process (shown as kinetic regime 1 in Fig. 3). In fact, the crystallised mass M_c increases linearly and rapidly during the early stage of the growth process. In the second region (shown as kinetic regime 2 in Fig. 3), M_c increases at a slower pace when compared to that of the first region, eventually reaching a plateau once all the supersaturation is consumed. Additionally, in this region the increasing crystallised mass exponentially decays with respect to time before reaching the saturation limit. This trend can be correlated with the supersaturation which is being
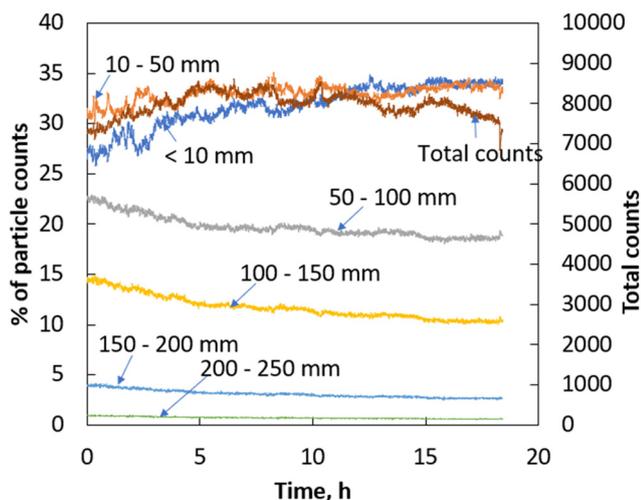

Fig. 5 Percentage of different size fractions of the crystals measured using FBRM *versus* time and the total FBRM counts *versus* time.

consumed during the growth process. During the early stage, the crystals start to grow from a highly supersaturated solution (in this case, S = 4.77). According to Fick's law of diffusion, the higher the concentration gradient, the faster the transfer of mass from the solution phase to the solid phase. This explains the faster crystal growth rate observed during the early stages of crystallisation.

If we define the crystallisation rate, k is defined as the slope in the plot of mass crystallised *versus* time, then we can estimate the crystallisation rate for both kinetic regions observed in Fig. 3. At 15 °C the mass of curcumin crystallised onto a unit mass of seed crystals increases rapidly with respect to time at a rate of 0.0086 g g^{-1} min^{-1} for the first 700 min and after that, the crystallisation increases at a much slower rate (~0.0019 g g^{-1} min^{-1}) and eventually reaches the saturation limit at ~2500 min. At 20 °C, the crystallisation rate increases rapidly at a rate of 0.0114 g g^{-1} min^{-1} for the first 500 min and after that the crystallisation rate increases at a slower rate of 0.0037 g g^{-1} min^{-1} and the solid concentration reaches the saturation limit at approximately 2000 min. A similar effect was observed during the crystal growth of curcumin at 38 °C, the solid concentration increases rapidly at a rate of ~0.048 g g^{-1} min^{-1} for the first 100 min and after which the crystallisation rate increases at a slower rate of 0.0064 g g^{-1} min^{-1} and finally reaches the saturation at ~800 min. It is clear from Fig. 3 that in both kinetic regions, the rate of crystallisation increases with the increase in temperature. The activation energy was calculated for the crystal growth in the observed two kinetic regions using the Arrhenius expression.

$$\ln(k) = \ln(k_o) - E/RT \tag{10}$$

where E is the activation energy, R is the universal gas constant, and k_o is the pre-exponential factor.

According to eqn (10), the activation energy of crystal growth and the preexponential factor can be calculated from the slope and intercept of the plot of ln (k) *versus* 1/T (shown in Fig. 6) Fig. 6 shows the activation energy calculated using eqn (10). For kinetic region 1 and 2, the activation energy for the crystal growth was estimated to be 57 and 35 kJ mol^{-1}, respectively.

The difference in the activation energy can be attributed to the crystal growth mechanism. Our recent work showed that curcumin tends to grow *via* the outgrowth of new crystalline units on the parent seed crystals at the expense of supersaturation followed by the growth of these newly formed crystals along with the parent seed crystals.[12] The activation energy of 57 kJ mol^{-1} can be attributed to the nonclassical crystal growth of curcumin (dictated by the repeated 2D nucleation) observed at higher supersaturation. On the other hand, the activation energy of 35 kJ mol^{-1} can be taken as the activation energy of the curcumin crystals grown *via* the classical crystal growth of the parent and the newly formed surface units. Earlier, Heffernan *et al.* reported on the surface free energy of nucleation for curcumin in
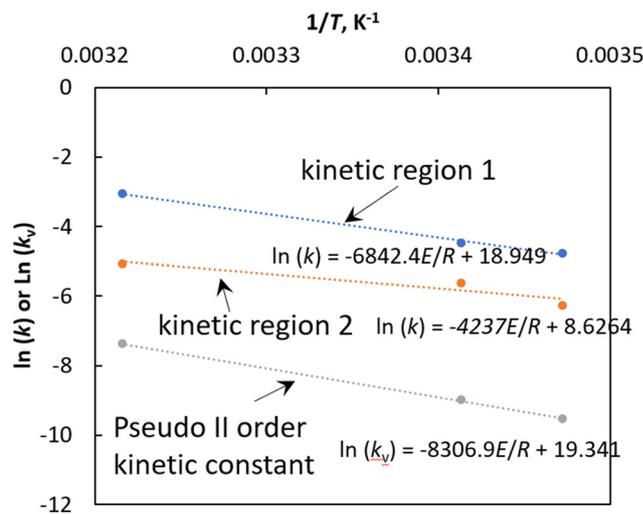

Fig. 6 ln(k) or ln(k_v) *versus* 1/T. The parameter 'k' refers to the slope of the plot of M_c *versus* t in the two different kinetic regions observed in Fig. 3. Note that k and k_v have different units. k: gram of curcumin per gram of seeds per minute and k_v: gram of seeds per gram of curcumin per minute.

isopropanol.[15,16] Using these values, we calculated the ΔG for the homogeneous nucleation of curcumin which was found to be in the range of 20.8 to 39.7 kJ mol^{-1} depending on the initial supersaturation. Likewise, in other work, Heffernan *et al.* reported a value of 38 J mol^{-1} for the activation energy associated with the classical growth of a spherical shaped curcumin.[16,17] Our results show that the activation energy of curcumin associated with the non-classical crystal growth dictated by the repeated 2D nucleation and the classical crystal growth of curcumin seems to be comparable with that of the Gibbs free energy of homogeneous nucleation and the activation energy of the spherical shaped curcumin reported in the literature, respectively.

3.3. Crystal growth of curcumin according to the pseudo second order kinetics

The overall crystallisation rate was predicted using the pseudo second order expression given by eqn (7). To do this, a nonlinear regression analysis was used to obtain the kinetic constant, k_v and the maximum number of active sites involved in crystallisation. For nonlinear regression analysis we minimised the error distribution between the experimentally obtained crystal growth kinetics and growth kinetics predicted by the pseudo second order kinetic expression. To minimise the error distribution, the solver function available within the Microsoft Excel was used by maximising the coefficient of determination r^2 between the experimental data and the predicted pseudo second order kinetics. The crystal growth kinetics predicted by the pseudo second order kinetics is shown in Fig. 3. It can be realised that the pseudo second order kinetics accurately predicts the crystal growth rate at the studied temperatures. The calculated kinetic constant, k_v, and the number of active sites

involved in the crystal growth, M^*, predicted by the pseudo second order kinetics and the corresponding error function value are given in Table 1. The $r^2 > 0.988$ confirms that the pseudo second order kinetics well predicts the crystal growth rate. It is worth mentioning that attempts were made to fit the experimental data with the multiple nucleation model (not shown here) which confirmed that it poorly represents the experimental data with r^2 values ranging from 0.0252 to 0.6278. Clearly, the r^2 values between the experimental data and the pseudo second order kinetics fits are remarkably high when compared to the r^2 values between the experimental data and the kinetics fits predicted by the conventional models like the birth and spread or the multiple nucleation model. Moreover, traditional models such as the multiple nucleation model necessitate the use of a shape factor to transform measurable parameters like supersaturation and mass crystallised into linear growth rates. This limitation hinders the application of such theoretical expressions in modeling the nonclassical crystal growth kinetics of curcumin. In that spirit, the pseudo second order kinetics is useful to model the nonclassical crystal growth kinetics associated with curcumin.

To gain additional insights, the effect of temperature on the kinetic constant obtained using the pseudo second order kinetics was analysed. The pseudo second order kinetic constant k_v increases with temperature. Here, we fixed the seed loading to 10 wt% of the theoretical mass that can be crystallised. This means that the number of active sites, M^* (defined as the mass of curcumin crystallised per unit mass of seed crystals), required for the crystal growth rate can be fixed to '10 g g^{-1} of curcumin seed crystals' irrespective of the working temperature or the theoretical mass that can be crystallised. The number of active sites required for crystal growth predicted by the pseudo second order kinetics is closer to the ones obtained by mass balance (see the M^* value shown in Table 1). The calculated k_v seems to vary with temperature following the Arrhenius expression.

$$\ln(k_v) = \ln(k_{vo}) - E/RT \quad (11)$$

Fig. 6 shows the plot of $\ln(k_v)$ versus $1/T$. The activation energy for crystal growth E and the preexponential factor k_{vo} were calculated from the slope and intercept of this plot using eqn (12). The activation energy of crystal growth

obtained based on the calculated pseudo second order kinetic expression was found to be ~69 kJ mol^{-1}. This value is slightly higher than the activation energy of crystal growth observed in kinetic region 1 and 2 (see Fig. 6). For comparison purposes, Table 2 shows the activation energy of crystal growth obtained based on the kinetic constants obtained from different theoretical models reported in the literature and the one obtained in this work for the crystal growth of curcumin in isopropanol. Table 2 also shows the mechanisms associated with the activation energy values reported in the literature.

The calculated activation energy associated with the curcumin crystals growing *via* the nonclassical crystal pathway seems to be comparable to the activation energy of crystal growth of calcium dihydrate sulfate and sucrose.[18,21] The activation energy of crystal growth in kinetic region 1 and 2 seems to be comparable to the crystal growth kinetics of active pharmaceutical ingredients that include paracetamol or acetaminophen, fenofibrate, carbamazepine, and risperidone in organic solvents. In terms of the initial crystallisation rate, v_k decreases globally with increasing temperature (see Table 1). It should be mentioned here that the observed decrease in initial crystallisation rate with respect to temperature is only due to the different M^* values at the studied temperature that deviates slightly from the ideal M^* value M^*_{ideal} obtained *via* a simple mass balance using the expression given in eqn (12)

$$M^*_{ideal} = (c_o - c^*)V/M_{seeds} \quad (12)$$

If the initial crystallisation rate is recalculated, based on the k_v values obtained from the pseudo second order expression and M^*_{ideal}, then it can be realised that $v_{initial}$ (see Table 1) increases linearly with the increase in temperature.

The k_v and v_k obtained from the pseudo second order kinetics vary with temperature and follow the following expression:

$$k_v = 251\,009\,162.4 \exp(-8306.9/T) \quad (13)$$

Eqn (13) is essentially the Arrhenius expression and can be used to predict k_v at different temperatures in Kelvin units. The outcomes indicate a pre-exponential factor of a considerable magnitude, specifically 10^8 g g^{-1} min^{-1}, for the crystal growth of curcumin in isopropanol.

Table 1 Pseudo second order kinetic parameters for the nonclassical crystal growth of curcumin in isopropanol

T, °C	k_v, g g^{-1} min^{-1} of curcumin seeds	M^*, g g^{-1}	v_k, g g^{-1} min^{-1} of curcumin seeds	M^*, sites g^{-1} of seeds	v_k,[a] g g^{-1} min^{-1} of curcumin seeds	r^2
15	7.30×10^{-5}	13.62	1.36×10^{-2}	2.26×10^{22}	7.30×10^{-3}	0.992
20	1.26×10^{-4}	12.44	1.95×10^{-2}	2.06×10^{22}	1.26×10^{-2}	0.988
38	6.26×10^{-4}	11.15	7.78×10^{-2}	1.85×10^{22}	6.26×10^{-2}	0.992

[a] v_k obtained assuming $M^* = M^*_{ideal}$. Note: for convenience we expressed the mass crystallised onto a unit mass of seed crystals expressed in terms of g g^{-1} of curcumin seeds. If we assume that each molecule of the target molecule occupies one site in the bulk crystal, it is possible to express M^* in terms of the number of sites involved in the crystal growth using the relation: $M^* \times 6.023 \times 10^{23}$ per molecular weight of curcumin.

Table 2 Activation energy values of crystal growth for different crystalline materials

Compound	E, kJ mol^{-1}	Theoretical model[a]	Ref.
Crude curcumin	69	Pseudo second order	This work
Calcium sulfate dihydrate	63	Power law	18
Potassium nitrate	31	Power law	19
Piracetam	45	Power law	20
Fenofibrate	36	Power law	20
Phenylbutazone	27	Power law	20
Acetaminophen	47	Power law	20
Carbamazapine	38	Power law	20
Risperidone	38	Power law	20
Sucrose	66.6	Surface diffusion	21
Sucrose	73	Spiral nucleation model	22
n-Hexatriacontane	29–49	Surface diffusion	23
Paracetamol [010] face	34	Linear law	24
Paracetamol [001] face	46	Linear law	24
Piracetam polymorphs	39–66	Power law	25

[a] The theoretical models used to obtain the activation energy.

It is worth mentioning here that eqn (13) is obtained based on the crystal growth experiments performed with a solution of initial supersaturation S = 4.77 and a seed loading of 10 wt%. A seed loading of 10 wt% means it is simply, M^*_{ideal} = 10 g g^{-1}. If we assume M^* in eqn (7) is equal to M^*_{ideal} then using eqn (7) and (11), it is possible to predict the crystal growth kinetics (provided they all are performed with a solution of initial supersaturation S = 4.77) at unknown temperatures. For demonstration purposes and as a proof of concept, we estimated the mass of curcumin crystallised onto a unit mass of seed crystals M_c at five different temperatures, 5, 10, 25 and 30 °C and the predicted kinetics are shown in Fig. 7. Here, we also showed the experimentally obtained M_c *versus* supersaturation S at 38 °C and the kinetics predicted

by the pseudo second order kinetics. Fig. 7 shows that if we know the relation of the pseudo second order kinetic constant as a function of temperature, then it can be used to predict the crystal growth kinetics. We performed all the crystal growth experiments for a fixed seed loading and fixed initial supersaturation. If we have additional information about the kinetic parameters obtained as a function of different operating variables that include seed loading, seed size, initial supersaturation and agitation speed, then it is possible to generate multiple correlations relating the kinetic parameters with these variables. Such correlations should allow prediction of the crystal growth kinetics of curcumin as a function of a wide range of operating variables.

3.4. Predicting the overall crystal growth kinetics using the pseudo second order expression

In the previous sections, a pseudo second order kinetic expression was used to predict the kinetic constant, M^* and ν_k. The predicted kinetic constants were used to predict the crystal growth kinetics without requiring any information about the shape factor. This means that the proposed model can be used to predict the crystal growth kinetics of seed crystals that do not retain the shape factor during the crystal growth process. Furthermore, the growth kinetics is expressed in terms of the mass crystallised onto a unit mass of seed crystals instead of the conventional overall growth rate or the linear growth rate. However, it should me mentioned here that the M_c obtained using the pseudo second order kinetic model can be transformed into the overall growth rate or linear growth rate, provided that the shape factors are known and it is assumed that there is no change in crystal habit during the growth process. To demonstrate this, in Fig. 8a we showed the experimentally obtained overall growth rate R_g (g cm^{-2} min^{-1}) as a function of supersaturation at 38 °C and compared the result with the R_g values predicted using the pseudo second order kinetic expression (see the Experimental section for the calculation
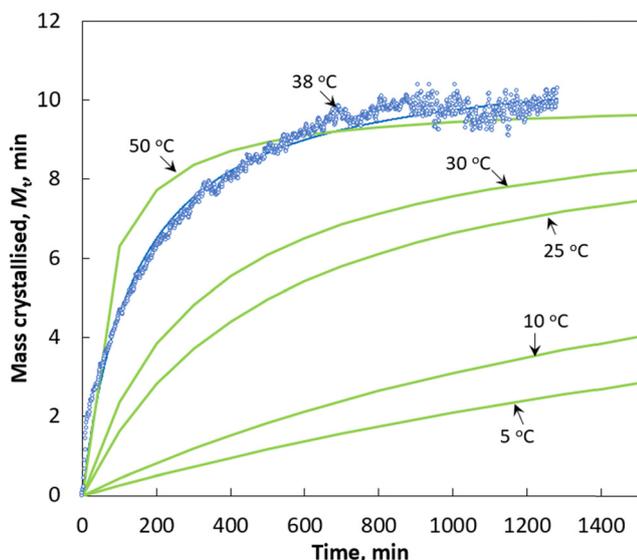

Fig. 7 Pseudo second order kinetics to predict the kinetics of nonclassical crystal growth of curcumin as a function of temperature (open blue circles: experimental data, solid blue lines best-fit pseudo second order kinetics, green lines: pseudo second order kinetics).
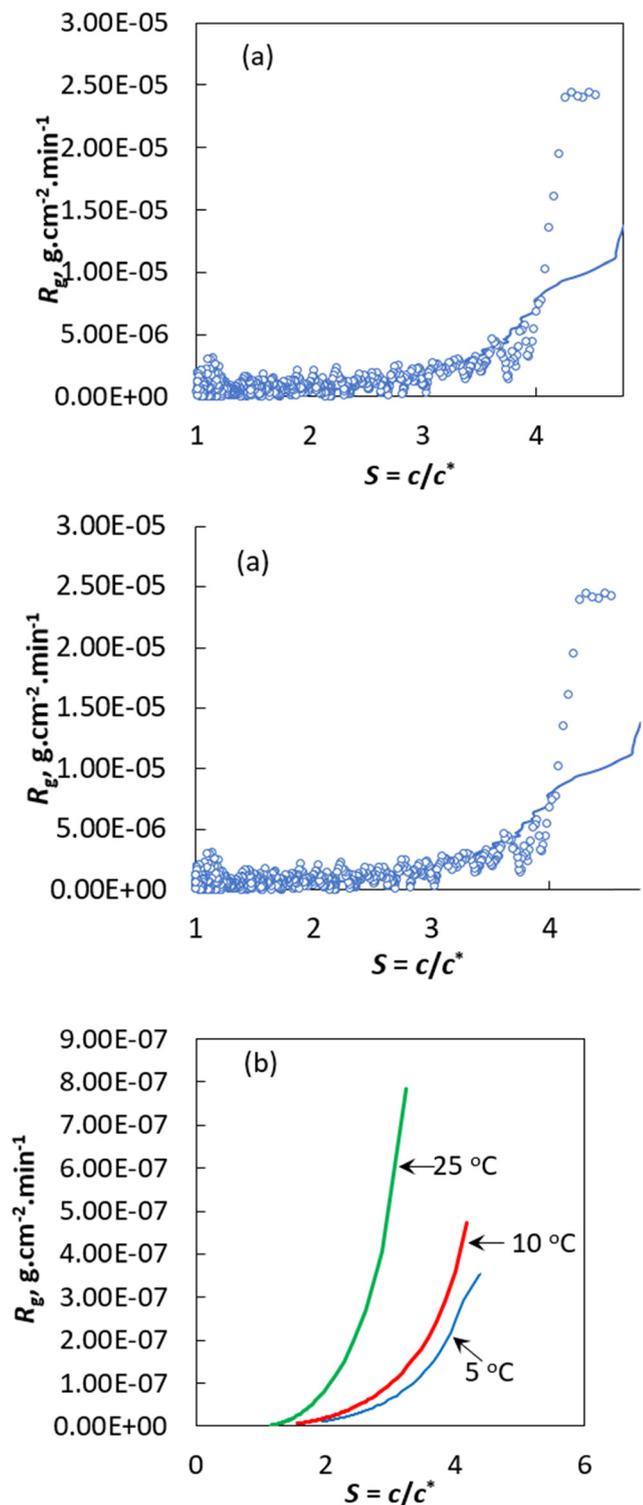
Fig. 8 (a) R_g of curcumin *versus* S at 38 °C (open blue circle: experimental data and blue solid line: pseudo second order kinetics). (b) R_g under new experimental conditions predicted using the pseudo second order kinetics.

procedures). The R_g value was obtained assuming that there is no change in the crystal shape factor, which is far away from reality if SEM images of the final crystals collected from

the experiments performed at different temperatures are considered. Nevertheless, the intention here was to demonstrate that the pseudo second order kinetics can predict the overall crystal growth rate of bulk crystals that grow following the rules of the classical crystal growth theory. The pseudo second order kinetics successfully predicts the R_g value obtained from the experiments at 38 °C. More importantly, the pseudo second order kinetics can be used to obtain the overall growth and linear growth rate of curcumin crystals. This means that the proposed pseudo second order kinetics can be used to predict the crystal kinetics of the crystal growth process, even if the growth follows the rule of the classical crystal growth kinetics (*i.e.*, each crystal facet in the bulk crystal will grow at a fixed rate and thus maintain the equilibrium crystal habit of a single crystal during the growth process).

Additionally, if an empirical correlation is obtained that relates the pseudo second order kinetic parameters with operating variables, then it is possible to obtain the overall growth kinetics under new experimental conditions. Solely for illustrative purposes, Fig. 8b depicts the projected overall growth rate of curcumin under new experimental conditions (*i.e.*, conditions not experimentally studied). Using eqn (13) and the pseudo second order expression the R_g of curcumin was predicted at 5, 10 and 25 °C. Accordingly, R_g increases with supersaturation and temperature.

4. Conclusions

The results clearly show that the crystal growth kinetics of curcumin can be predicted accurately by using the pseudo second order kinetics. The pseudo second order kinetics can be an excellent model to predict the kinetics of a nonclassical crystal growth process. The pseudo second order kinetics also predicts several useful parameters related to the crystal growth kinetics, which include the overall growth kinetic constant, maximum number of active sites required for crystal growth and initial crystallisation rate. The results also confirmed that it is possible to predict the activation energy associated with the crystal growth process using the pseudo second order kinetics. If required, it is possible to use the approach to predict the overall growth kinetics or the linear growth rate.

5. Experimental

5.1. Materials

Crude curcumin was purchased from Merck (curcumin >75% nominal purity), containing <5 wt% bisdemethoxy curcumin (BDMC) and <20 wt% dismethoxy curcumin (DMC). HPLC-grade IPA (>99.9%) was purchased from Arcos Organics Aldrich. The high-performance liquid chromatography experiments performed show that curcumin is 78.6% pure and contains <18 wt% DMC and <4 wt% BDMC. Curcumin was used as received for the crystallisation experiments.

5.2. Preparation of CUR seed crystals

Seed crystals were prepared using microwave assisted cooling crystallisation experiments. Seeds were purposely prepared *via* crystallisation under microwave irradiation, as our experience shows that flawless and agglomeration free single crystals with a needle habit can be obtained *via* microwave irradiated crystallisation. For this, an automatic microwave reactor was used (ATPIO XO-SM100, 0–1000 W). Crystallisation experiments were performed with a reactor volume of 50 mL; 0.3 g of pure curcumin was dissolved in 50 mL of isopropanol-2 at 75 °C using microwave for 10 min. Then the solution was cooled to a working temperature of 20 °C at a cooling rate of 8 °C min^{-1}. Once the solution reached the working temperature, the reactor temperature was set to 20 °C for 2 h and the jacket temperature was set to 5 °C for 2 h. This set temperature difference between the jacket temperature and the reactor temperature allowed us to maintain the microwave environment throughout the crystallisation experiment. Once the solution reached 20 °C, we observed primary nucleation in less than 2 min. After 2 h, we collected the final crystals *via* filtration using Whatman filter paper (no. 1). The filtered crystals were then dried using an oven maintained at a temperature of 60 °C for 24 h. The obtained crystals were used as such as seeds in the crystal growth experiments.

5.3. Process analytical technology (PAT) assisted crystal growth experiments

Crystal growth experiments were performed in batch mode using a 100 mL Easymax workstation. All the crystal growth experiments were performed using the 100 mL reactor. All the crystal growth experiments were performed using a recipe programmed using Mettler Toledo's iControl software. The temperature inside the crystalliser was maintained or altered by an external jacket that relies on electrical heating and solid-state cooling technology. The agitation inside the crystalliser in all the experiments was maintained at 250 rpm and the agitation was provided using an overhead stirrer. *In situ* Raman spectroscopy was used to monitor the suspension density inside the crystalliser.

Isothermal de-supersaturation crystal growth experiments were performed by adding a known mass of crude curcumin into 78.6 g of isopropanol. All solids were dissolved by heating the solution to 75 °C at a rapid heating rate. Then the solution was maintained at 75 °C for 45 min to ensure complete dissolution of curcumin. Then the solution was cooled down to the working temperature at a fixed cooling rate of 8 °C min^{-1} to generate a supercooled solution, $\Delta T = T^* - T_w$ or supersaturated solution. The term T^* refers to the solubility temperature and T_w is the working temperature. Once the solution reached the working temperature, the seeds were added immediately. The supersaturation was defined in terms of the ratio of the concentration of curcumin in the solution to the solubility concentration at the working temperature, $S = c/c^*$. In this work, we performed three experiments at 15, 20 and 38 °C. The maximum working temperature T_w was fixed to 38 °C, considering the solubility of curcumin in isopropanol. To generate a supersaturated solution at $T_w > 38$ °C, which is sufficient to initiate the crystal growth, heating the solution to near the boiling point of the solvent is required. For safety purposes, the experiments were designed such that the solution temperature is always ~15 °C lower than the boiling point of the solvent. The lowest working temperature of 15 °C was fixed based on the recommended operating temperature in industry. Crystallisation at $T_w < 15$ °C involves an energy penalty associated with the cost required to bring the solution temperature from 75 °C to T_w, which should be avoided. For all the crystal growth experiments, the initial supersaturation was fixed to $S = c/c^* = 4.77$. In all the crystallization experiments, the solution was maintained at the working temperature for ~24 h which is sufficient to achieve complete saturation. We fixed the number of active sites that will be involved in the crystal growth rate to 10:10 g g^{-1} of curcumin seeds. This was achieved by maintaining the seed percentage to 10 wt%.

5.4. Predicting the solubility using *in situ* Raman spectroscopy

Solubility experiments were performed using a 100 mL volume reactor Easymax workstation. 78.6 g of isopropanol was added to reactor and the reactor temperature was set to 3 °C. Once the reactor temperature reached 3 °C, a known mass of curcumin was added into the reactor. The reactor temperature was maintained at 3 °C for 10 min, after this, the reactor temperature was increased to 70 °C at a very slow heating rate of 0.078 °C min^{-1}. As the temperature increases, the concentration of curcumin in solvent increases, whereas the concentration of solids in the solution tends to decrease. The suspension density was monitored using *in situ* Raman spectroscopy for every 1 min for the entire duration of the experiment. At the end of the experiment (once the reactor temperature reached 70 °C), from each spectrum collected at different time intervals, three intense Raman peaks were selected positioned at ~1251 cm^{-1} (corresponding to the C–O stretching of curcumin), ~1431 cm^{-1} (corresponding to the phenol C–O stretching of curcumin) and ~1601 cm^{-1} to quantify the suspension density in the solution.[11] Based on the observed peak intensity at different temperatures, the solubility was obtained using the procedures described in section 3.1.

5.5. Determination of solid concentration using Raman spectroscopy

The suspension density was monitored using *in situ* Raman spectroscopy. A RX1 Raman spectrometer supplied from Kaiser Optical System, Inc. (Ann Arbor, MI, USA) was used to collect the Raman spectra. A ¼th inch immersion probe which is connected to the spectrometer *via* a fibre-optic cable was used to collect backscattered radiation from the

sample. The probe was positioned roughly 2 cm above the bottom of the base of the crystallizer, with the power at the sample being approximately 150 mW. Using iC Raman software (Mettler Toledo), a measurement region of 150–3425 cm^{-1} at 786 nm excitation laser was utilised with a spectral resolution of 4 cm^{-1} to collect the spectra which were averaged over 30 scans using an exposure time of 2 s.

We used a calibration free method to correlate the Raman intensity with the supersaturation ΔC with the mass crystallised M_t at any time, t:[11]

$$\Delta c = c - c^* = (I_t - I_o)/(I_o - I_f) \times M_c \tag{14}$$

$$M_t = M_c - \Delta c \tag{15}$$

where:

$\Delta c = c - c^*$ at any instant of time (g L^{-1}); M_c (g L^{-1}) is the mass that can be crystallized or theoretical yield. The value of M_c can be obtained from a simple mass balance based on the initial experimental conditions and solubility at the working temperature ($M_c = (c_o - c^*)/V$). I_o is the intensity of the Raman peak when time $t = 0$. This value should correspond to the intensity of the Raman peak of the completely dissolved solution (i.e., no solids). I_t is the intensity of the Raman peak at any instant of time during crystallization and I_f is the intensity of the Raman peak observed at complete saturation due to the crystal growth. For crystal growth experiments, from each spectrum collected at different time intervals, the intense peak at ~1601 cm^{-1} was chosen corresponding to the aromatic vibration $C = C_{ring}$ of curcumin to quantify the suspension density in the solution.[11] As this peak more quickly responds to a change in the solid-phase concentration it was chosen. Following eqn (15), the ratio of the peak intensity with respect to the peak intensity of the solvent was found to be linearly proportional. The peak intensity of curcumin here refers to the height of this band from the two-point baseline that connects 1617 cm^{-1} and 1571 cm^{-1} in the Raman spectra.[11]

For the solubility experiments, from each spectrum collected at different time intervals, three intense peaks were selected at 1251 cm^{-1} (corresponding to the C–O stretching of curcumin), 1431 cm^{-1} (corresponding to the phenol C–O stretching of curcumin) and 1601 cm^{-1} to quantify the suspension density in the solution.[11] As this peak more quickly responds to a change in the solid-phase concentration it was chosen. Following eqn (12), the ratio of the peak intensity with respect to the peak intensity of the solvent was found to be linearly proportional.

5.6. Microscopic analysis

The morphology of the final crystals was analysed using a scanning electron microscope (SEM). The solid samples were transferred onto the carbon tape pasted on the SEM stage. Samples were then coated with gold for 1 min, and the images were obtained using an SU70 Hitachi FEG-SEM instrument.

5.7. Calculation of the crystal growth rate

The linear growth rate can be obtained using a simple mass balance. The linear or overall growth kinetics of crystals can be estimated from the change in the mass of crystals, Δm, with respect to a given interval Δt.

For any time, interval Δt, the linear growth rate of curcumin crystals, R, (cm min^{-1}) considering constant supersaturation, was given by:[1,12,22,26,27]

$$R = \frac{M_{final}^{1/3} - M_{initial}^{1/3}}{(f_v \rho_c N)^{1/3} \Delta t} \tag{16}$$

M_{final} and $M_{initial}$ are the mass of final and initial crystals in the crystallizer corresponding to the time interval Δt, f_v and ρ_c are the volume shape factor and density of the curcumin crystals, respectively, and t is the time. N is the number of growing crystals.

If we assume that there is no crystal breakage or agglomeration, then N is a constant and can be predicted using the expression:[1,22,26,27]

$$N = \frac{m_o}{f_v \rho_c L_o^3} \tag{17}$$

where m_o (g) and L_o (cm) represent the mass and characteristic size of seed crystals, respectively. L_o was determined based on the average length (maximum Feret diameter) of at least 30 000 seed crystals using MorphologiG3 and was found to be approximately equal to 8×10^{-3} cm.

The overall growth rate, R_g, (g cm^{-2} min^{-1}) can be determined from eqn (16) after introducing the shape factors for the curcumin crystals:[1,22,26,27]

$$R_g = 3 \frac{f_v \rho_c}{f_s} R \tag{18}$$

The term f_s is the area shape factor. In this study, f_v and f_s are 0.01 and 0.42, respectively, while the curcumin density, ρ_c, is 1.3 g cm^{-3}.

5.8. Useful correlations required to predict the overall growth kinetics using pseudo second order kinetic parameters

The solution supersaturation Δc at any time t can be obtained using the expression:

$$c_o - c = \frac{M_t M_{seeds}}{V} \tag{19}$$

Eqn (17) can be used to calculate the theoretical yield by replacing M_t with M^*.

It should be remembered that the solid concentration in the crystalliser corresponds to the sum of mass of seeds and the mass of curcumin crystallised onto a unit mass of seed crystals. Thus, the actual mass of the crystals, M_{actual} (g L^{-1}),

inside the crystals in grams at any time t can be obtained using the expression (can be obtained by performing a simple mass balance):

$$M_{actual} = \frac{M_t M_{seeds}}{V} + M_{seeds} \qquad (20)$$

where M_t can be obtained using the pseudo second order kinetic expression given in eqn (7), and M_{seeds} is the mass of the seeds added to the crystalliser expressed in g L^{-1}.

To obtain the overall growth kinetics, R_g using pseudo second order kinetics, the M_{final} and $M_{initial}$ in eqn (18) should be replaced with the mass of crystals (M_{actual}) obtained using eqn (20).

Conflicts of interest

There are no conflicts to declare.

Acknowledgements

References

1 J. W. Mullin, *Crystallization*, ed. J. W. Mullin, ISBN 9780750648332, Butterworth-Heinemann, 4th edn, 2001.

2 A. Mersmann, *Crystallization Technology Handbook*, CRC Press, 1st edn, 2001.

3 K. H. Hsi, M. Kenny, A. Simi and A. S. Myerson, *Cryst. Growth Des.*, 2013, **13**, 1577–1582.

4 J. Chen, B. Sarma, J. M. B. Evans and A. S. Myerson, *Cryst. Growth Des.*, 2011, **11**, 887–895.

5 W. K. Burton, N. Cabrera and F. C. Frank, *Philos. Trans. R. Soc., A*, 1951, **243**, 299–358.

6 A. A. Chernov, *Sov. Phys., Usp.*, 1961, **4**, 116.

7 K. V. Kumar, *Ind. Eng. Chem. Res.*, 2009, **48**, 7852–7859.

8 K. Vasanth Kumar, *Ind. Eng. Chem. Res.*, 2009, **48**, 11236–11240.

9 P. Sanphui and G. Bolla, *Cryst. Growth Des.*, 2018, **18**, 5690–5711.

10 P. Sanphui, N. R. Goud, U. B. R. Khandavilli, S. Bhanoth and A. Nangia, *Chem. Commun.*, 2011, **47**, 5013–5015.

11 K. V. Kumar, K. A. Ramisetty, K. R. Devi, G. R. Krishna, C. Heffernan, A. A. Stewart, J. Guo, S. Gadipelli, D. J. L. Brett, E. P. Favvas and Å. C. Rasmuson, *ACS Omega*, 2021, **6**(37), 23884–23900.

12 K. Vasanth Kumar, S. Gadipelli, K. A. Ramisetty, C. Heffernan, A. A. Stewart, V. Ranade, C. Howard and D. Brett, *CrystEngComm*, 2023, **25**, 3361–3379.

13 C. Cliffe, A Principal Attempt to Break the Stochastic Nature of Nucleation, *Bachelor's Final Year Research Project*, University of Limerick, 2021.

14 K. Vasanth Kumar, *Ind. Eng. Chem. Res.*, 2009, **48**(10), 5105–5110.

15 C. Heffernan, M. Ukrainczyk, J. Zeglinski, B. K. Hodnett and Å. C. Rasmuson, *Cryst. Growth Des.*, 2018, **18**, 4715–4723.

16 C. Heffernan, An investigation into the effect of impurities on the crystallization of curcumin, *PhD Thesis*, University of Limerick, 2019.

17 C. Heffernan, R. Soto, B. K. Hodnett and Å. C. Rasmuson, *CrystEngComm*, 2020, **22**, 3505–3518.

18 S. T. Liu and G. H. Nancollas, *J. Cryst. Growth*, 1970, **6**, 281–289.

19 J. E. Helt, Effects of supersaturation and temperature on nucleation and crystal growth in a MSMPR crystalliser, *PhD thesis*, Iowa State University, 1976.

20 R. Soto, V. Verma, A. Lynch, B. K. Hodnett and Å. C. Rasmuson, *Cryst. Growth Des.*, 2020, **20**, 7626–7639.

21 L. D. Shiau, *Chem. Eng. Sci.*, 2003, **58**, 5299–5304.

22 K. V. Kumar and F. Rocha, *Surf. Sci.*, 2010, **604**, 981–987.

23 R. J. Davey, *J. Cryst. Growth*, 1986, **76**, 637–644.

24 B. Y. Shekunov, M. E. Aulton, R. W. Adama-Acquah and D. J. W. Grant, *J. Chem. Soc., Faraday Trans.*, 1996, **92**, 439–444.

25 R. Soto and Å. C. Rasmuson, *Cryst. Growth Des.*, 2019, **19**, 4273–4286.

26 K. Vasanth Kumar, Transfer of impurities into crystals in industrial processes: Mechanism and kinetics, *PhD thesis*, University of Porto, 2010.

27 J. Garside, J. W. Mullin and S. N. Das, *Ind. Eng. Chem. Process Des. Dev.*, 1973, **12**, 369–371.